Facile In Situ Synthesis of Noble Metal Nanoparticles in Porous Cellulose Fibers

Junhui He,† Toyoki Kunitake,*,† and Aiko Nakao‡

Frontier Research System and Surface Characterization Division, The Institute of Physical and Chemical Research (RIKEN), Hirosawa 2-1 Wako, Saitama, 351-0198 Japan

Received August 4, 2003. Revised Manuscript Received September 12, 2003

In situ synthesis of noble metal (Ag, Au, Pt, Pd) nanoparticles was carried out under ambient conditions in porous cellulose fibers as nanoreactors. Particles of less than 10 nm were readily prepared using the described approach, and monodisperse nanoparticles were obtained under an optimized concentration of the metal precursor solution. The nanoporous structure and the high oxygen (ether and hydroxyl) density of the cellulose fiber constitute an effective nanoreactor for in situ synthesis of metal nanoparticles. The nanopore is essential for incorporation of metal ion and reductant into cellulose fibers as well as for removal of unnecessary byproducts from fibers. This was endorsed by negligible adsorption of metal ion onto nonporous films of poly(vinyl alcohol) and starch. The ether oxygen and the hydroxyl group not only anchor metal ions tightly in cellulose fibers via ion−dipole interactions, but they also stabilize metal nanoparticles by strong bonding interaction with their surface atoms. The preparative procedure is facile and versatile, and provides a simple route to manufacturing of useful noble metal nanoparticles.

Introduction

Direct synthesis of nanoparticles in solid matrixes is attracting increasing interest in terms of practical applications and synthetic challenges. For example, carbon-supported Pt nanoparticles were prepared and tested as a catalyst for fuel cells.[1] Multilayered polymer films[2] and block copolymer films[3] were used as nanoreactors for formation of silver nanoparticles. Noble metal nanoparticles were synthesized in mesoporous silica films[4] and in ultrathin nanoporous TiO_2 films.[5] Silver particles of narrow size distribution were produced upon reversible chemical transformation between metallic and oxide states in the titania matrix[6] and in mesoporous silica that was grafted with hydrophobic $Si(CH_3)_3$ groups at the pore surface.[7]

We have shown recently that amorphous nanoporous TiO_2 films can accommodate various metal ions via ion exchange.[8] These metal ions are readily converted to metallic nanoparticles by reduction with H_2 plasma and $NaBH_4$. It is worthy of notice that ligand-free metallic nanoparticles are stably kept in the TiO_2 matrix. The stability probably arises from strong bonding interaction between the surface atoms of the nanoparticle and the surrounding oxygen atoms of the TiO_2 matrix,[9] as also demonstrated for the stabilization of a Ti metal cluster.[10] This crown ether effect would be expected for other oxygen-rich matrixes.

Chart 1. Structure of Cellulose Chain

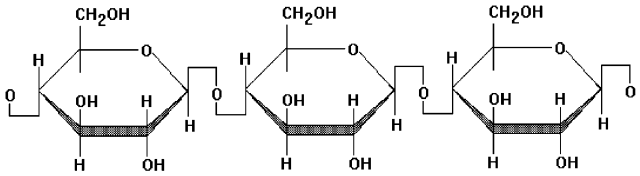

Cellulose is an oxygen-rich natural carbohydrate (polysaccharide) consisting of anhydroglucose units joined by an oxygen linkage to form a linear molecular chain (Chart 1). Recently, iron (3−15 nm) and copper nanoparticles (30−120 nm) were prepared in cellulose acetate films by first mixing iron or copper complexes and cellulose acetate in tetrahydrofuran followed by coating the mixture on substrate and reduction of metal complexes to nanoparticles with H_2 at elevated temperatures. These nanoparticle-containing cellulose acetate films demonstrated catalytic activities in hydrogenation of olefins, CO oxidation, NO reduction, and water-gas shift reaction under relatively mild conditions.[11] These polymer films are nonporous, and catalytic sites may

* To whom correspondence should be addressed. E-mail: kunitake@ruby.ocn.ne.jp.
† Frontier Research System.
‡ Surface Characterization Division.

(1) (a) Zhou, Z.; Wang, S.; Zhou, W.; Wang, G.; Jiang, L.; Li, W.; Song, S.; Liu, J.; Sun, G.; Xin, Q. *Chem. Commun.* **2003**, 394−395. (b) Xu, Z.; Qi, Z.; Kaufman, A. *Chem. Commun.* **2003**, 878−879.
(2) Joly, S.; Kane, R.; Radzilowski, L.; Wang, T.; Wu, A.; Cohen, R. E.; Thomas, E. L.; Rubner, M. F. *Langmuir* **2000**, *16*, 1354−1359.
(3) Horiuchi, S.; Fujita, T.; Hayakawa, T.; Nakao, Y. *Langmuir* **2003**, *19*, 2963−2973.
(4) (a) Plyuto, Y.; Berquier, J.-M.; Jacquiod, C.; Ricolleau, C. *Chem. Commun.* **1999**, 1653−1654; (b) Guari, Y.; Thieuleux, C.; Mehdi, A.; Reyé, C.; Corriu, R. J. P.; Gomez-Gallardo, S.; Philippot, K.; Chaudret, B.; Dutartre, R. *Chem. Commun.* **2001**, 1374−1375.
(5) He, J.; Ichinose, I.; Kunitake, T.; Nakao, A. *Langmuir* **2002**, *18*, 10005−10010.
(6) He, J.; Ichinose, I.; Fujikawa, S.; Kunitake, T.; Nakao, A. *Chem. Commun.* **2002**, 1910−1911.
(7) Besson, S.; Gacoin, T.; Ricolleau, C.; Boilot, J.-P. *Chem. Commun.* **2003**, 360−361.
(8) He, J.; Ichinose, I.; Fujikawa, S.; Kunitake, T.; Nakao, A. *Chem. Mater.* **2002**, *14*, 3493−3500.
(9) He, J.; Ichinose, I.; Kunitake, T.; Nakao, A.; Shiraishi, Y.; Toshima, N. *J. Am. Chem. Soc.* **2003**, *125*, 11034−11040.
(10) Franke, R.; Rothe, J.; Pollmann, J.; Hormes, J.; Boennemann, H.; Brijoux, W.; Hindenburg, Th. *J. Am. Chem. Soc.* **1996**, *118*, 12090−12097.

10.1021/cm034720r CCC: $25.00
Published on Web 10/22/2003

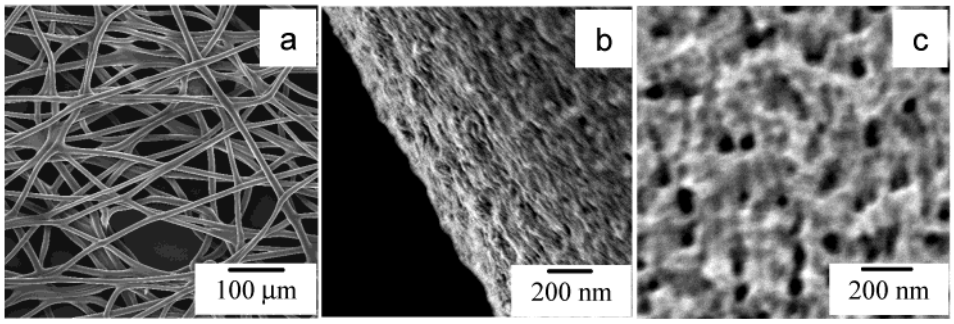

Figure 1. FE-SEM images of the texture of PS-2 (a), the edge (b) and surface (c) of a single cellulose fiber.

not be fully accessible by guest molecules. In addition, the formation of large particles as shown above was apparently caused by aggregation of smaller metal particles. It is obvious that a decrease in particle sizes would significantly enhance catalytic activities.[9]

Natural cellulose fibers have a porous structure and are composed of microfibrils of 10−30-nm width that are three-dimensionally connected with each other.[12] Their specific surface areas were reported to be in the range of 30−55 $m^2\ g^{-1}$.[13] Very recently, wood (bamboo and cedar) was used as a template for creating zeolites by void filling, revealing the complex pore morphology within cellulose fibers.[14] Such morphological features may provide a unique reaction vessel for synthesizing nanoparticles, allowing much enhanced access of guest molecules to catalytic centers, compared with nonporous films.

In this work, we report on surprisingly facile synthesis of noble metal nanoparticles of less than 10 nm in diameter and with narrow size distribution by using porous cellulose fibers as unique nanoreactor as well as particle stabilizer.

Experimental Section

Lint-free cellulose papers (49 μm thick, PS-2, Bemcot, 100% cellulose, Asahi Kasei, Japan) and filter papers (288 μm thick, Toyo Roshi Kaisha, Japan) were used as the sources of cellulose fibers. $AgNO_3$, $Pd(NO_3)_2$, and $NaBH_4$ were purchased from Kanto Chemical. $AuCl_3$ was obtained from Aldrich and $PtCl_4$ from Merck-Schuchardt. Poly (vinyl alcohol) (PVA, MW ~78 000) and soluble starch were obtained from Polysciences and Wako Pure (Japan), respectively. All these chemicals were guaranteed reagents and used as purchased. Ultrapure water with the specific resistance of 18.3 MΩ·cm was obtained by reversed osmosis followed by ion-exchange and filtration (Yamato-WQ500, Millipore, Japan).

Noble metal ions were impregnated into cellulose fibers by immersing them in aqueous $AgNO_3$, $AuCl_3$, $PtCl_4$, or $Pd(NO_3)_2$ of appropriate concentrations for 1 min, followed by rinsing with ethanol for ca. 30 s. After the fibers were reduced in aqueous $NaBH_4$ (200 mM) for 10 min and rinsed in pure water for 1 min, the obtained specimens were dried overnight in a vacuum at room temperature.

Nonporous PVA film was fabricated layer-by-layer by immersing a piranha-solution (H_2SO_4/H_2O_2 3:1) cleaned quartz plate in an aqueous solution (25 °C) containing 100 unit mM PVA and 2 M NaCl for 15 min, followed by rinsing twice with pure water (1 min each) and drying with N_2 gas.[15] Twenty cycles were repeated and the obtained film was estimated to be ca. 22 nm thick. Nonporous starch film was spin-coated on a quartz substrate from aqueous starch (5 mg/mL). Individual spin-coating was carried out at 3000 rpm for 2 min using 200−250 μL of aqueous starch. After 4 cycles of spin-coating, the total thickness was estimated to be ca. 20 nm.

UV−visible absorption spectra were recorded with pure PS-2 paper as the reference on a Shimadzu UV-3100PC UV−Vis−NIR scanning spectrophotometer. X-ray photoelectron spectroscopy (XPS) measurements were carried out on an ESCALAB 250 (VG) using Al Kα (1486.6 eV) radiation. The applied power was operated at 15 kV and 20 mA. The base pressure in the analysis chamber was less than 10^{-8} Pa. Smoothing, background removal, and peak fitting were carried out with a VG analysis software package, ECLIPS. All the peaks were corrected with the C 1s peak (C−O, carbon from cellulose) at 286.5 eV as the reference. Scanning electron microscopy (SEM) observations were carried out on a Hitachi S-5200 field emission scanning electron microscope at 1 kV after sputtering <2-nm Pt particles on sample surfaces by a Hitachi E-1030 ion-coater. Transmission electron microscopy (TEM) observations were carried out on a JEOL JEM-2000EX instrument. Histogram, mean diameter, and standard deviation were obtained by sampling 100 metal nanoparticles in TEM images of 3×10^5 magnification, followed by analyses using SigmaPlot 2001.

Results and Discussion

Formation of Silver Nanoparticles in Porous Cellulose Fibers. Lint-free cellulose papers (49 μm thick) were used first as the source of cellulose fibers. They are composed of uniform cellulose fibers of ca. 11-μm width, as shown in Figure 1a. The surface of the fiber is rough (Figure 1b) and consists of pores of diameter of 30−70 nm (Figure 1c). These nanopores may allow guest molecules to penetrate into their inner spaces. Thus, when a piece of PS-2 paper was immersed in aqueous $AgNO_3$ (1 min), silver ions were readily impregnated into the cellulose fibers through the pores. Most of the incorporated Ag^+ ions were bound to cellulose macromolecules probably via electrostatic (i.e., ion−dipole) interactions, because the electron-rich oxygen atoms of polar hydroxyl and ether groups of cellulose are expected to interact with electropositive transition metal cations.[11,16] Rinsing by ethanol (ca. 30 s) effectively removed those Ag^+ ions that were not

(11) (a) Shim, I.-W.; Choi, S.; Noh, W.-T.; Kwon, J.; Cho, J. Y.; Chae, D.-Y.; Kim, K.-S. *Bull. Korean Chem. Soc.* **2001**, *22*, 772−774. (b) Shim, I.-W.; Noh, W.-T.; Kwon, J.; Cho, J. Y.; Kim, K.-S.; Kang, D. H. *Bull. Korean Chem. Soc.* **2002**, *23*, 563−566.
(12) Mark, H. F., Kroschwitz, J. I., Eds. *Encyclopedia of Polymer Science and Technology*; John Wiley & Sons: New York, 1985; Vol. 3, p 60.
(13) Kaewprasit, C.; Hequet, E.; Abidi, N.; Gourlot, J. P. *J. Cotton Sci.* **1998**, *2*, 164−173.
(14) Dong, A.; Wang, Y.; Tang, Y.; Ren, N.; Zhang, Y.; Yue, Y.; Gao, Z. *Adv. Mater.* **2002**, *14*, 926−929.
(15) Serizawa, T.; Hashiguchi, S.; Akashi, M. *Langmuir* **1999**, *15*, 5363−5368.
(16) Kesting, R. *J. Appl. Polym. Sci.* **1965**, *9*, 663−688.

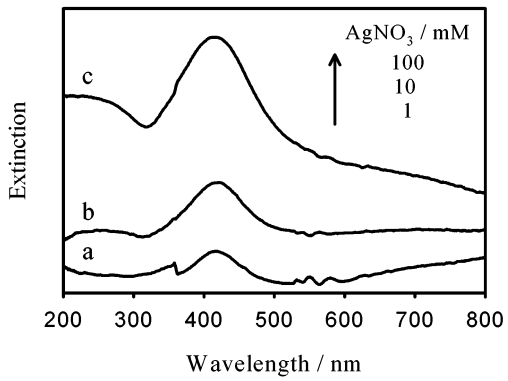

Figure 2. Absorption spectra of silver nanoparticles in PS-2 cellulose fiber. The nanoparticle was prepared from aqueous $AgNO_3$ of 1 mM (a), 10 mM (b), and 100 mM (c) (three curves were vertically shifted for comparison).

anchored to cellulose fibers. After reduction in aqueous $NaBH_4$ (200 mM) and rinsing with pure water, the original colorless cellulose paper turned bright yellow (shown later in Figure 4a and b). The yellow color probably resulted from the plasmon absorption of Ag nanoparticles. In contrast, no changes were observed by FE-SEM at high magnifications in the surface morphologies of cellulose fibers.

XPS spectra of the above product showed a C 1s peak with binding energy at 286.5 eV, characteristic of carbon bonded to oxygen in cellulose macromolecules. The XPS and Auger peaks of Ag were found at 368.1 eV ($3d_{5/2}$) and 1130.4 eV, respectively, from which the modified Auger parameter (α) was calculated to be 724.3 eV. This is in agreement with that of metallic silver (726.1 eV),[5,6] indicating that Ag^+ ions were effectively converted to their metallic states. The atomic ratio of silver to oxygen was also estimated to be 1.0:100 by the corrected peak intensities of XPS spectra. Thus, the molar ratio of silver to the glucose unit is 1:20 in the current specimen.

The color of cellulose paper with Ag particles changed from light yellow to bright yellow to deep yellow with increasing concentrations of aqueous $AgNO_3$ from 1 mM to 10 mM to 100 mM. Figure 2 shows UV−visible extinction spectra of these Ag/cellulose products with pure PS-2 cellulose paper as the reference. Because the same cellulose paper was used as the reference, the extinction spectra may be considered as the absorption of Ag species, although porous cellulose matrix can strongly scatter the incident light. At 1 mM, a narrow symmetrical absorption band is located at 417 nm, and is attributable to the surface plasmon resonance of silver nanoparticles in agreement with the observed yellow color. No absorption was observed at wavelengths longer than 500 nm (Figure 2, curve a). This implies that small Ag nanoparticles of narrow size distribution were formed. The surface plasmon peak underwent a red-shift to 424 nm and was slightly broadened at 10 mM $AgNO_3$ (Figure 2, curve b). At a still higher concentration of 100 mM $AgNO_3$, the surface plasmon absorption becomes much broadened, along with appearance of broad absorption in the range of 500−800 nm (Figure 2, curve c). As the plasmon peak is still located at 414 nm for this sample, both small and large Ag particles (wide size distribution) are probably formed. It is noted that the absorption intensity of the plasmon band increases with the concentration of aqueous $AgNO_3$, in agreement with the color changes. This is attributed to the increase of the silver loading.

These conclusions are supported by TEM observations. The cellulose paper with Ag nanoparticles was cut into pieces, dispersed in pure water, transferred onto a SiO-coated copper grid with dispenser, dried in a vacuum overnight, and observed by TEM. As shown in Figure 3a and d, virtually monodisperse Ag nanoparticles were obtained at 1 mM $AgNO_3$. Their mean diameter (d) and standard deviation (σ) were estimated to be 4.4 and 0.2 nm, respectively. At 10 mM $AgNO_3$ (Figure 3b and e), the particle size slightly increases (d = 4.8 nm) and the size distribution becomes broadened (σ = 1.2 nm). The size of the Ag nanoparticle is much larger (d = 7.9 nm) and the particle size distribution becomes rather wide (σ = 2.4 nm) at 100 mM $AgNO_3$ (Figure 3c and f). Therefore, it is possible to control the size and size distribution by adjusting the concentration

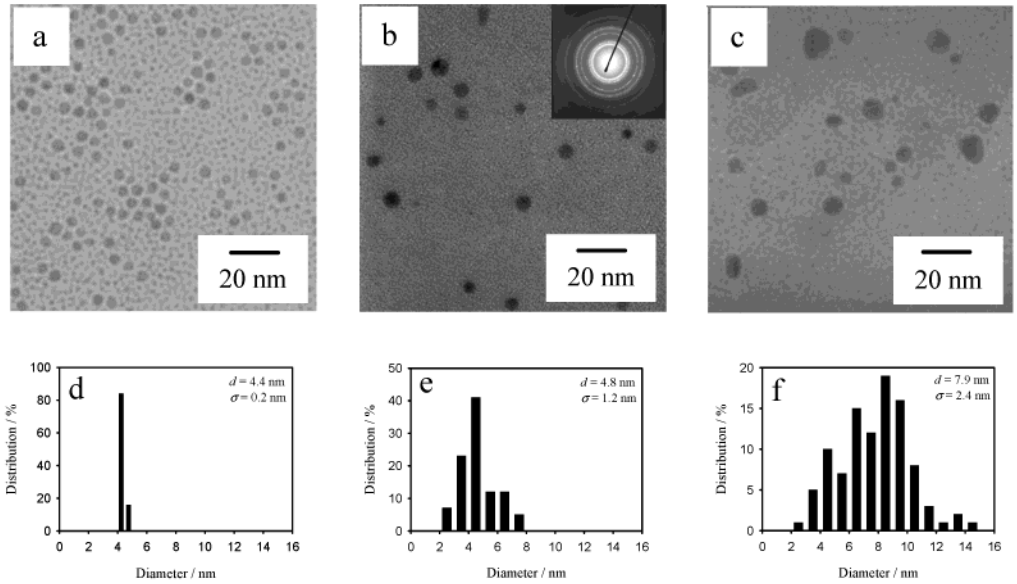

Figure 3. TEM images (a−c) and histograms (d−f) of silver nanoparticles in PS-2 cellulose fiber prepared from aqueous $AgNO_3$ of 1 mM (a, d), 10 mM (b, e), and 100 mM (c, f).

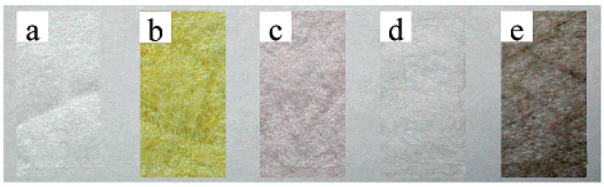

Figure 4. Cellulose specimens with (a) none, (b) Ag, (c) Au, (d) Pt, and (e) Pd metallic nanoparticles.

of metal ions in solution. Electron diffraction experiments revealed a clear pattern of five rings that correspond to (111), (200), (220), (311), and (331) planes of cubic Ag crystals (Figure 3b, insert). It is undoubted that the particles were well crystallized.

Because of the nanoporous structure of cellulose fiber and strong interactions between Ag^+ ions and the hydroxyl and ether groups of cellulose macromolecule, silver ions were uniformly and tightly anchored to the cellulose fibers. Such interactions would lower the mobility of Ag^+ ions, enhance the formation of silver nuclei, and prevent the growth of larger particles. This is particularly true at low Ag^+ ion concentrations, and explains formation of monodisperse Ag nanoparticles (after $NaBH_4$ reduction) under such conditions. At higher $AgNO_3$ concentrations, larger amounts of Ag^+ ions are adsorbed on cellulose fibers, leading to large and widely distributed particles after reduction.[5] It was previously reported that organic solvents such as tetrahydrofuran can effectively stabilize Ti clusters in the zerovalent state via the Ti−O bonding interaction.[10] In the current system, it is expected that the hydroxyl and ether groups may also play an important role in stabilization of metal nanoparticles in addition to the nanoporous structure of cellulose fiber.

Preparation of Other Noble Metal Nanoparticles. The versatility of the current approach was tested by synthesis of other noble metal nanoparticles, such as gold, platinum, and palladium. Aqueous solutions of gold trichloride ($AuCl_3$), platinum tetrachloride ($PtCl_4$), and palladium nitrate ($Pd(NO_3)_2$), each 10 mM, were used as the precursor solution and the same procedure was employed for particle synthesis. The final products showed different colors (Figure 4), though no morphological changes were observed by FE-SEM. A light pink PS-2 sheet was obtained for gold (Figure 4c), a colorless one was obtained for platinum (Figure 4d), and a dark gray one was obtained for palladium (Figure 4e). Apparently, these colors are related to plasmon absorptions of the corresponding metal nanoparticles. The XPS peaks of Au, Pt, and Pd appeared at 83.8 eV (Au $4f_{7/2}$), 70.8 eV (Pt $4f_{7/2}$), and 334.9 eV (Pd $3d_{5/2}$). These data are in agreement with the metallic data of Au, Pt, and Pd, respectively,[5,6] and support the formation of respective metal nanoparticles. The molar ratios of Au, Pt, and Pd to the glucose unit in cellulose were estimated by XPS to be 1:118, 1:143, and 1:6, respectively. Thus, under the identical concentration of metal ions, the loading might be influenced not only by their valences, but also other factors such as equilibrium and dissociation, etc.

The formation of metal nanoparticles was confirmed by TEM observations. Figure 5 shows TEM images and histograms of metal nanoparticles. The presence of Au (Figure 5a), Pt (Figure 5b), and Pd (Figure 5c) nanoparticles is clearly seen. The Au particle is small, with mean diameter and standard deviation of 3.0 and 0.7 nm, respectively (Figure 5d). The particle size and standard deviation for Pt were estimated to be 5.7 and 2.2 nm, respectively (Figure 5e), and they were 6.2 and 1.5 nm for palladium, respectively (Figure 5f). The metal/glucose ratio and the size/size distribution of the obtained metal nanoparticles were further compared at the same concentration of metal ion for all four noble metal elements. The results showed that the smaller the metal/glucose ratio, the smaller the nanoparticle and the narrower the size distribution, except for Pt element. This trend agrees with that found in Figures 2 and 3. Thus, the loading of metal ion may play a more important role than its valence.

Preparation of Metal Nanoparticles in Fractured Cellulose Fibers. The cellulose fibers in the PS-2 paper maintain original morphologies. In contrast, cellulose fibers in filter paper are mechanically fractured. The fractured fibers in filter paper also show a

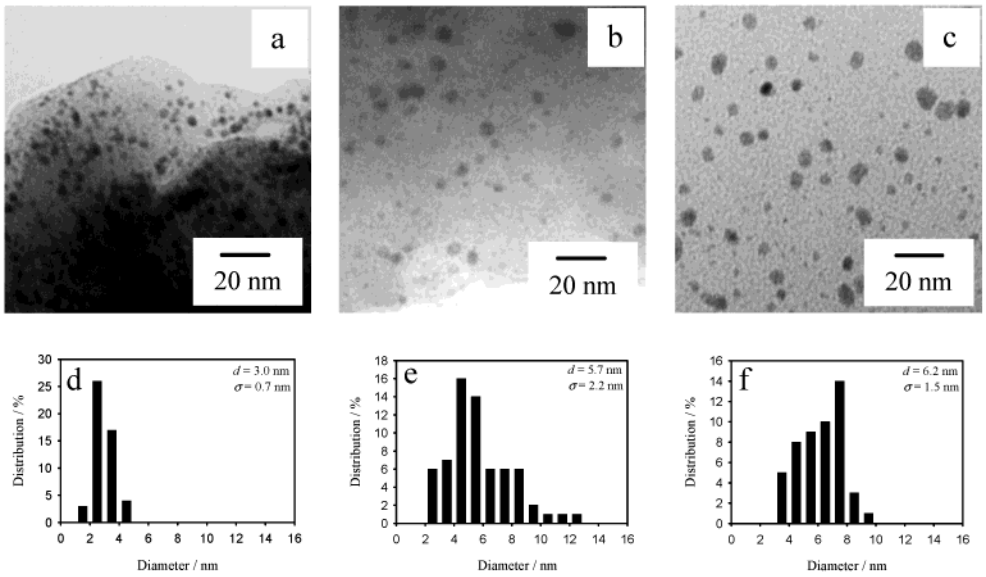

Figure 5. TEM images and histograms of Au (a, d), Pt (b, e), and Pd (c, f) nanoparticles in PS-2 cellulose fiber. They were prepared using 10 mM $AuCl_3$, $PtCl_4$, and $Pd(NO_3)_2$ in water.

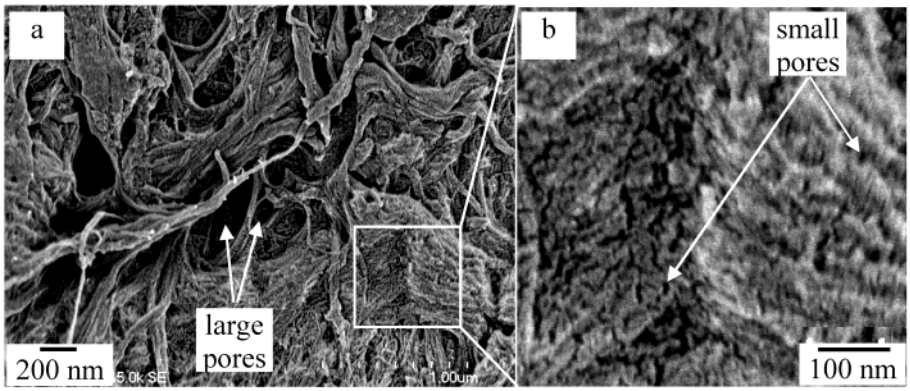

Figure 6. (a) Typical FE-SEM image of fractured cellulose fibers and (b) magnified image of highlighted area in (a). Arrows in (a) point to large pores, and those in (b) point to small pores.

hierachical structure, as shown in Figure 6. It contains large pores of submicron width (Figure 6a). The magnified area shows small pores on the nanoscopic scale (Figure 6b). These pores are formed by interconnected microfibrils. As discussed above, small pores may be used to anchor nanoparticles and large pores can serve as channels for migration of reactants and products. Ag nanoparticles were synthesized in these cellulose fibers under the identical conditions. As shown in Figure 7, Ag nanoparticles were formed and anchored on the surface or in the amorphous part[12] of microfibrils. However, they were unlikely to be formed within the crystalline part of microfibrils. Figure 7a, b, and c are three areas in a TEM grid with minced cellulose fibers containing Ag nanoparticles. The average size and the size distribution were estimated to be 4.0 and 1.4 nm, respectively, from their histogram (Figure 7d). These results are similar to those (d = 4.8 nm, σ = 1.2 nm) obtained for PS-2 cellulose fibers under the identical conditions, indicating that the fractured cellulose fibers provide a similar environment for impregnation of metal ions and formation of metal nanoparticles.

Attempted Formation of Metal Nanoparticles in Nonporous Films. To clarify the role of the porous structure of cellulose fibers for the formation of metal nanoparticles, nonporous films of PVA and starch were used as the matrix for formation of Ag nanoparticles. A nonporous PVA film with thickness of ca. 22 nm was fabricated in the layer-by-layer fashion from aqueous PVA (100 unit mM) containing 2 M NaCl, as described in the literature.[15] Such films were nonporous, and there exists strong hydrogen bonding interaction among PVA chains. When the same preparative procedure as we employed for porous cellulose fibers was applied to this thin film, the amount of Ag nanoparticles formed in the film was negligibly small, as indicated by UV−visible absorption spectroscopy (an absorbance of 0.002 at 417 nm was recorded). A nonporous starch film of ca. 20 nm thickness was tested in a similar way, but a negligibly small absorbance (0.001 at 415 nm) was recorded. These small plasmon absorptions may be attributed to surface-attached Ag nanoparticles formed from surface-adsorbed Ag^+ ions. Thus we conclude that the porous structure of cellulose fibers is indispensable for efficient incorporation of metal ions and subsequent formation of metal nanoparticles.

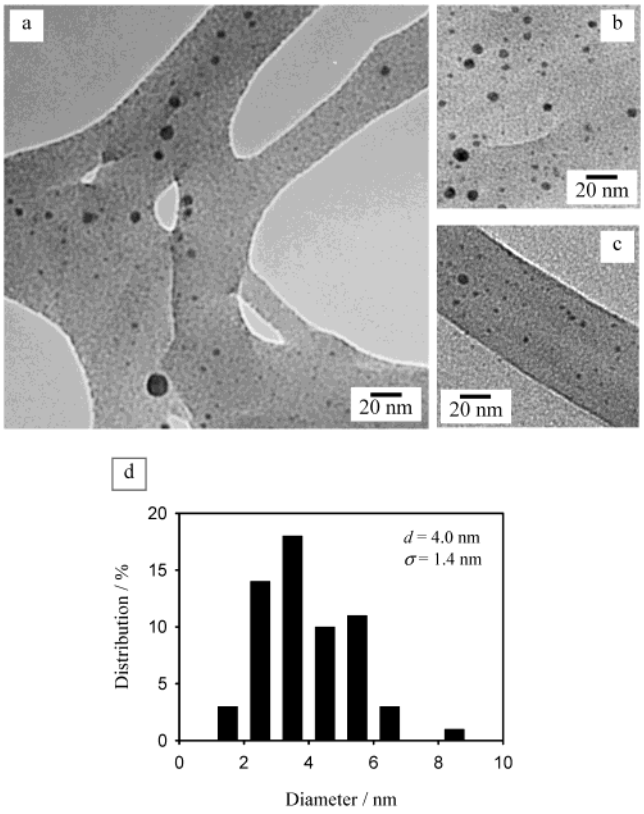

Figure 7. TEM images of silver nanoparticles in fractured cellulose fibers of filter paper prepared from aqueous $AgNO_3$ of 10 mM. Images (a), (b), and (c) were obtained at three different locations in a given TEM grid, and (d) is their histogram.

Concluding Remarks

To summarize, we succeeded in direct synthesis of noble metal nanoparticles in porous cellulose fibers. The size and size distribution are controllable by adjusting synthetic parameters such as the concentration of metal ion. Under optimized conditions, monodisperse metal nanoparticles were obtained. The implication of the present results is at least 2-fold. First is that the nanoporous structure and the high oxygen (ether and hydroxyl) density of cellulose fibers constitute an effective nanoreactor for in situ synthesis of metal nanoparticles. The nanopore is essential for introduction of metal ion and reductant into cellulose fibers and removal of unnecessary byproducts from fibers. The ether oxygen and the hydroxyl group not only anchor metal

ions tightly onto cellulose fibers via ion−dipole interactions, but also stabilize metal nanoparticles by strong bonding interaction with their surface metal atoms. The porous cellulose fiber is analogous to nanoporous titania in this respect.[5,6,9] In the latter, oxygen atoms in the metal oxide network stabilize bare metal ions in a way similar to crown ethers, in which coordinating oxygen atoms are juxtaposed toward central metal ions. The metal nanoparticle formed after reduction is stabilized by a strong bonding interaction between the outermost orbitals of its surface atoms and the surrounding oxygen atoms of the TiO_2 matrix,[9] as also demonstrated for a Ti metal cluster.[10] A second implication is related to practical applications of such materials. Many practical uses of nanoparticles are made possible only in solid supports. This requirement is met without additional procedures in the current system. The preparative procedure is surprisingly simple. It can provide a facile approach toward manufacturing of metallic nanocomposites, antimicrobial materials, low-temperature catalysts, and other useful materials.

Acknowledgment. We are very grateful to Dr. S. Onoue for assisting in electron diffraction measurements and helpful discussion.

CM034720R